Nonlinear response of layer growth dynamics in the mixed kinetics–bulk-transport regime

Peter G. Vekilov, J. Iwan D. Alexander, and Franz Rosenberger*
Center for Microgravity and Materials Research, University of Alabama in Huntsville, Huntsville, Alabama 35899
(Received 1 April 1996)

In situ high-resolution interferometry on horizontal facets of the protein lysozyme reveal that the local growth rate R, vicinal slope p, and tangential (step) velocity ν fluctuate by up to 80% of their average values. The time scale of these fluctuations, which occur under steady bulk transport conditions through the formation and decay of step bunches (macrosteps), is of the order of 10 min. The fluctuation amplitude of R increases with growth rate (supersaturation) and crystal size, while the amplitude of the ν and p fluctuations changes relatively little. Based on a stability analysis for equidistant step trains in the mixed transport–interface-kinetics regime, we argue that the fluctuations originate from the coupling of bulk transport with nonlinear interface kinetics. Furthermore, step bunches moving across the interface in the direction of or opposite to the buoyancy-driven convective flow increase or decrease in height, respectively. This is in agreement with analytical treatments of the interaction of moving steps with solution flow. Major excursions in growth rate are associated with the formation of lattice defects (striations). We show that, in general, the system-dependent kinetic Peclet number, Pe_k, i.e., the relative weight of bulk transport and interface kinetics in the control of the growth process, governs the step bunching dynamics. Since Pe_k can be modified by either forced solution flow or suppression of buoyancy-driven convection under reduced gravity, this model provides a rationale for the choice of specific transport conditions to minimize the formation of compositional inhomogeneities under steady bulk nutrient crystallization conditions. [S1063-651X(96)11912-7]

PACS number(s): 81.10.Aj, 47.20.Bp, 68.35.Ct, 87.90.+y

I. INTRODUCTION

Externally imposed modulations of crystal-growth conditions typically result in compositional and structural variations (zoning, banding, striations) in the crystals [1]. Growth rate fluctuations and resulting striations can, however, also occur under quasisteady conditions during melt solidification in geological environments [2–4] and externally stable laboratory experiments [5,6], as well as in electrocrystallization [7], physical vapor transport [8], and inorganic solution growth processes [9–12]. Recently we found that such intrinsic fluctuations also exist in protein crystallization and possess a characteristic time scale of O (10 min) [13].

Theoretical treatments of intrinsic growth rate fluctuations have been based on both macroscopic and microscopic models. In the macroscopic approaches, the species fluxes and, thus, growth rates are assumed to be governed by coupled bulk transport and interfacial processes. Their rates depend, respectively, linearly and nonlinearly on concentration(s). Nonlinearities in interfacial kinetics can be due to chemical reactions that precede or compete with incorporation into the crystal [2,3,14], impurity effects [15,16], or a delay in the interface response to a perturbation in the local concentration of a component [4]. The coupling of linear and nonlinear steps results in unsteady rates with time constants largely exceeding those of the individual steps [17–19]. The general trend that emerges from the above models is schematically illustrated in Fig. 1; see also Ref. [4]. If growth proceeds under pure kinetics or transport control, where the interfacial concentration C_s approaches, respectively, the bulk concentration C_∞ and equilibrium concentration (solubility) C_{eq}, the system is stable, i.e., perturbations decay rapidly. For mixed control, however, the system is unstable. Perturbations lead to fluctuations about a mean growth rate. Maximum response occurs if the weights of kinetics and transport in the overall rate control are comparable.

Numerous microscopic models for unsteady growth involve the formation, stability, and decay of step bunches (macrosteps). Stimulated by detailed observations of various step patterns [20,21], dynamic step bunching has been associated with surface diffusion [22–25] and different kinetic coefficients for incorporation into a step from the upper and lower terraces (Schwoebel effect [26]). Of particular importance for our investigation is an analysis of the stability of an equidistant step train under diffusive solute bulk transport conditions [27]. The authors assumed that the diffusion layer width δ is growth rate independent, as in rapid forced solu-

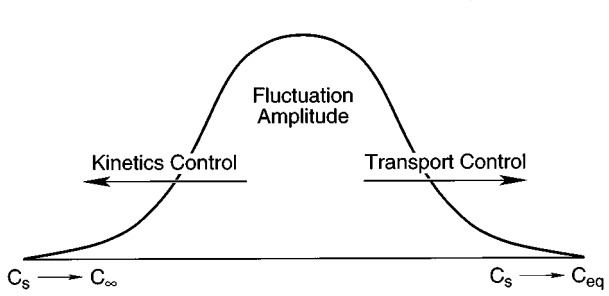

FIG. 1. Schematic presentation of the dependence of rate fluctuation amplitude on the coupling between transport and interface processes, after Ref. [4]. Under either pure kinetics or transport control, when the interfacial solute concentration C_s approaches, respectively, the bulk or equilibrium concentration (C_∞ or C_{eq}), perturbations decay.

*Corresponding author.

tion flows [28,29], and that the solute concentration in the solution increases linearly with distance from the growing facet. For these conditions it was found that step bunching occurs only in response to perturbations with wavelength λ greater than a critical value

$$\lambda_c = 2\pi\left[\frac{\Gamma}{s_b}\left(\frac{D}{\beta_0}+\delta\right)\right]^{1/2}, \tag{1}$$

with the capillary constant

$$\Gamma = \Omega\alpha/k_B T \tag{2}$$

(Ω is the molecular volume in crystal, and α the surface free energy), solute diffusivity D, kinetic coefficient of the face with an equidistant step train β_0, and concentration supersaturation in the bulk $s_b=(C_\infty - C_{\rm eq})/C_{\rm eq}$. The wavelength of the most rapidly developing perturbation is

$$\lambda_{\max} = \sqrt{3}\lambda_c . \tag{3}$$

Equation (1) identifies the kinetic Peclet number

$$\mathrm{Pe}_k = \beta_0\delta/D, \tag{4}$$

i.e., the relative weight of kinetics and transport, as the parameter governing stability. Under both pure kinetic ($\beta_0\to 0$, $\mathrm{Pe}_k\to 0$) and transport control ($\delta\to\infty$, $\mathrm{Pe}_k\to\infty$), $\lambda_c\to\infty$. Thus, similar to the general behavior depicted in Fig. 1, no step bunching is predicted to occur in response to perturbations of any wavelength. Of course, this linear stability analysis cannot predict the magnitude and temporal characteristics of the ensuing finite amplitude fluctuations. This can only be the subject of a parametric analysis that takes into account the specific layer generation mechanism and interstep interaction through a microscopic nutrient supply field. Such efforts are underway in our group. However, evaluations of Eqs. (4) and (1) [see Sec. IV B] show that typically Pe_k is finite and λ_c is of the order of 10 μm. Hence, for any macroscopic crystal size, equidistant step trains are unstable. Since the formation of macrosteps is typically associated with inclusion and defect formation [30,31], the growth of large and structurally homogeneous crystals usually requires intensive stirring of the solutions. This, as we will see below, is because convective nutrient fluxes in direction opposite to that of step motion can reduce the formation of macrosteps (step bunching).

The interaction of step trains with convective-diffusive solute transport has been analyzed in Refs. [32–36.] It was found that convective flow affects the development of macrosteps if

$$u_\infty \gg \nu_{\rm ph} \tag{5}$$

and

$$u_\infty\lambda_0/D > 1, \tag{6}$$

where u_∞ is the bulk solution flow velocity parallel to the interface, and $\nu_{\rm ph}$ is the phase velocity of the step density wave with wavelength λ_0. For order of magnitude estimates, $\nu_{\rm ph}$ is assumed to be comparable to the average step velocity $\overline{\nu}$. It is important to note that the relative direction plays a crucial role for the stability of the step train. Solution flow in the direction of step motion causes step bunching in response to perturbations with λ longer than

$$\lambda_c^f = 2.51\,\overline{p}^{3/2}\left(\frac{\delta D}{u_\infty}\right)^{1/2}, \tag{7}$$

where $\overline{p}$ is the average slope of the vicinal face considered [33]. Solution flow opposite to the step motion suppresses bunching. This behavior was observed in forced solution flow experiments with ammonium dihydrogen phosphate crystals [32].

Buoyancy-driven flow, which, due to solutal density gradients, is always present in solution growth systems under gravity, can also affect the stability of step trains. In most inorganic systems, however, inequality (5) does not hold in unstirred solutions. Typical u_∞'s are of the order of 100 μm/s [37], i.e., comparable to characteristic ν's [38,39]. In contrast, protein systems, due to their slow interface kinetics, could provide an opportunity to observe such interactions between natural convection and step motion. For instance, for lysozyme $\overline{\nu}$ is typically 0.05–0.5 μm/s [13,40,41], while u_∞'s are about 10 μm/s [42,43]. With this u_∞, $D=0.73\times 10^{-6}$ cm^2/s [44], and observed step bunching wavelength $\lambda_0=\overline{\nu}\Delta t$ of about 50 μm [13], Eq. (6) yields $u_\infty\lambda_0/D\approx 7$. Therefore, step trains should be affected by the buoyancy-driven flows. This should reduce the macrostep height along step trains moving from the center to the periphery of a horizontal facet since, in this case, the natural convection flow is opposite to the step motion [42,45]. On the other hand, as step bunches move toward the center of a horizontal facet, their height can be expected to increase. At the same time, evaluating Eq. (7) for lysozyme, with $\overline{p}=5\times 10^{-3}$ [40] and $\delta=200$ μm [42], yields a flow-induced critical wavelength $\lambda_c^f\approx 30$ cm. Since this is orders of magnitude larger than the typical crystal sizes of O (100 μm), it is unlikely that the fluctuations observed in our earlier work are due to flow-step train interactions.

In the following, we will identify the origin of these fluctuations through simultaneous observations of the time-dependent normal growth rate R, vicinal slope p, and tangential velocity ν, and their possible dependence on solution purity, supersaturation, crystal size, and direction of step motion with respect to solution flow. In addition, we will explore the consequences of these intrinsic fluctuations for crystal quality. For studies of the underlying *time-averaged* growth kinetics, and its dependence on step sources and impurities; see Refs. [40, 46].

II. EXPERIMENT

Solutions were prepared as described elsewhere [47,48], using lysozyme with three purity levels: (i) as supplied by Sigma and (ii) by Seikagaku, and (iii) a Seikagaku lysozyme purified to 99.9% with respect to higher molecular weight proteins [49]. Growth solution temperatures were stabilized to within ± 0.01 °C. Supersaturations were expressed as $\sigma=\ln[C/C_{\rm eq}(T)]$, where $C_{\rm eq}(T)$ is the solubility at the temperature T of the experiment [47]. For the interferometry setup (depth resolution $\sim$200 Å), data collecting and processing routines, and their testing to ensure reliable measure-

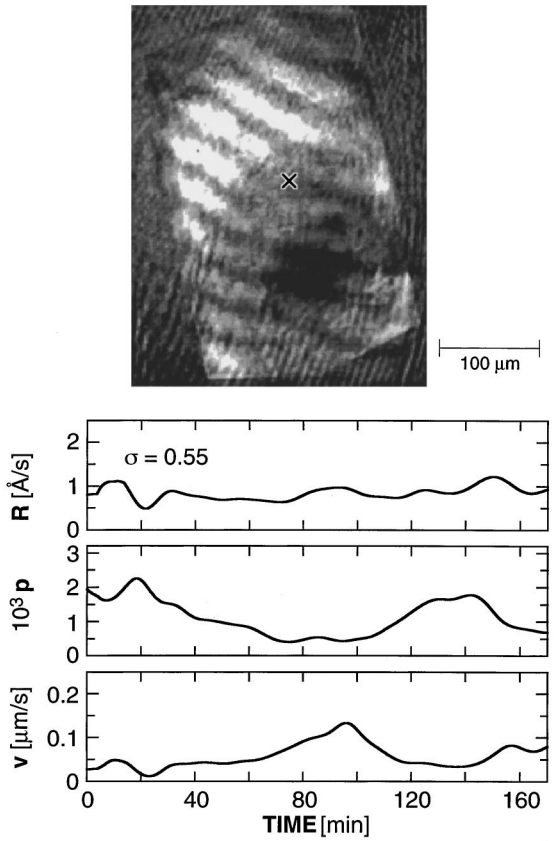

FIG. 2. Time traces of normal growth rate R, local slope p, and tangential (step) velocity ν, obtained at the marked location ($\times$) of the (110) facet shown in the interferogram. Steps generated by dislocation bunch outcropping in lower part of the facet; for details, see Ref. [40].

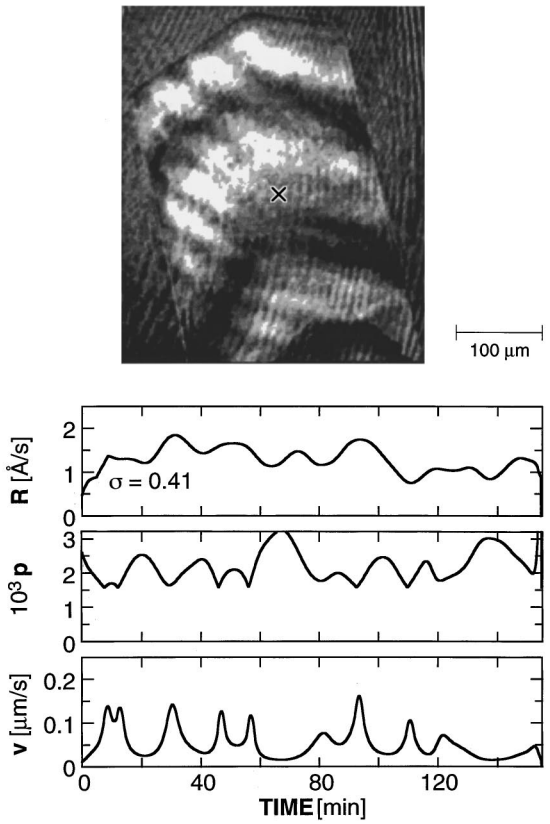

FIG. 3. Time traces of normal growth rate R, local slope p, and tangential (step) velocity ν, obtained at the marked location ($\times$) of the (110) facet shown in the interferogram. Steps generated by dislocation bunch outcropping below bottom of interferogram; for details, see Ref. [40].

ments of the temporal dependencies of the kinetic quantities, see Ref. [13]. Note that this technique simultaneously provides local values of R and p at several points of interest on the studied facet. The step velocity ν is then calculated from the relation

$$R(t)=p(t)\nu(t). \tag{8}$$

Due to the limitations in the experiment resolution, the local determinations of R represent integrals of the interferometric intensity over interfacial areas of $\sim 0.5\times 0.5\ \mu\text{m}^2$, while the p values are averaged over distances of $\sim 3\ \mu$m; see Ref. [13]. Both {110} and {101} tetragonal lysozyme faces were studied. No differences were found; hence, only results for the {110} faces are presented here.

III. RESULTS AND DISCUSSION

A. Fluctuations in R, p, and ν, and step source effects

Figures 2 and 3 show that the local growth rate R, vicinal slope p, and tangential velocity ν are not steady and fluctuate by as much as ~80% of their average values. The variations in p, which is proportional to the step density, indicate that the fluctuations are due to the passage of step bunches. Note that the excursions of p and ν tend to be in opposite directions: high and low step densities are associated, respectively, with low and high tangential velocity. This indicates strong overlap of the steps' nutrient supply fields, as also suggested by our earlier work on microscopic deviations from perfect planarity of the facets [50]. This step interaction is likely governed by overlapping surface diffusion fields [50,51]. Furthermore, we found no dependence of the fluctuations on solution purity for our system.

Figures 2 and 3 present fluctuation traces during the growth of the same crystal. The growth hillock shown in Fig. 3 is steeper and, correspondingly, the average slope is higher. Note that this is associated with higher fluctuation amplitudes. The steeper slope reflects a step source of higher activity, likely due to cooperation of a larger number of dislocations than in Fig. 2.

The characteristic fluctuation time Δt (average time between major excursions) is of O (10 min). For comparison, the characteristics step generation time $\tau_{\text{step}}=h/R$, with a step height h of at most a few hundred Å and an average growth rate R of some 10 Å/s, is of O (10 s). Hence, in contrast to the findings with barium nitrate and potash alum in, respectively, Refs. [10] and [12], the fluctuation times are at least several tens of times longer than τ_{step}. However, in another investigation, barium nitrate showed fluctuations in R with $1\ \text{min}<\Delta t<10\ \text{min}$ [9], which were interpreted in terms of moving multidislocation step sources of varying activity; see also Refs. [40,52,53]. In our investigations, Δt's obtained with two-dimensional (2D) nucleation- or

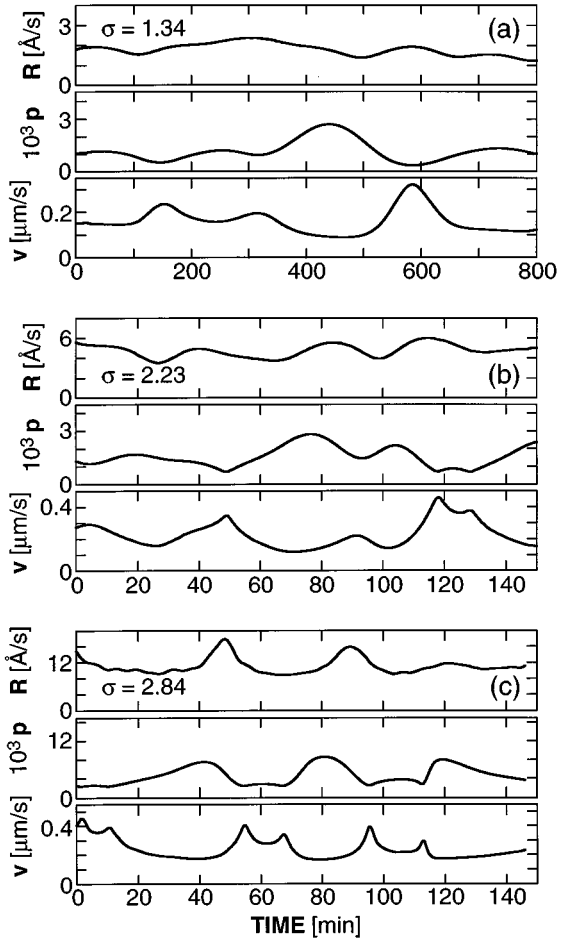

FIG. 4. Time traces of normal growth rate R, local slope p, and tangential (step) velocity ν recorded at facet center of same crystal at three different supersaturations. Layer generation by 2D nucleation; see Ref. [40]. Crystal size ~250 μm, increasing insignificantly during measurements due to slower growth of side faces.

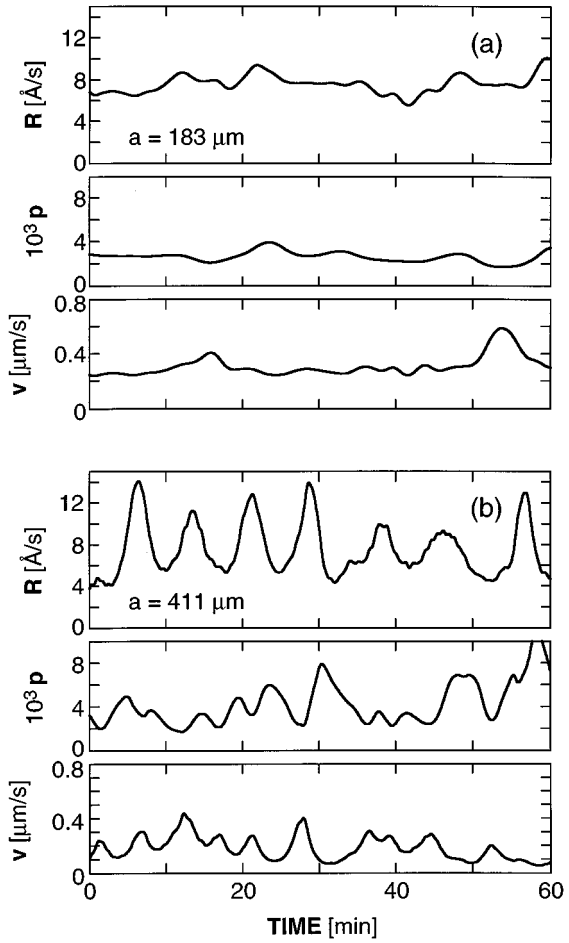

FIG. 5. Increase of fluctuation amplitude at facet center location with crystal size a, and step generation by 2D nucleation; σ=2.84.

dislocation-step sources were comparable. Therefore, we conclude that our fluctuations are not caused by the dynamics of multidislocation step sources, though they may be affected by them.

B. Supersaturation and crystal-size dependencies

Figure 4 presents fluctuation traces recorded at the same location of a crystal at increasing supersaturations. Note that the fluctuation amplitude of both p and ν is independent of σ. At low σ, $\nu(t)$ and $p(t)$ are largely in counterphase. With increasing σ, the phase difference between ν and p fluctuations becomes more random, and consequently the R excursions increase. We also see that the characteristic time of the fluctuations Δt (average time between major excursions) decreases with supersaturation. At σ=2.84 [Fig. 4(c)], Δt drops to 20–30 min. In other experiments at comparable or higher supersaturations, we observed Δt's as short as 5 min. In Fig. 5, we compare the fluctuations observed at a facet center for two different crystal sizes a. We see that the variations in R, p, and ν, and the fluctuation frequency, significantly increase with a.

Supersaturation (average growth rate) and crystal size are parameters that strongly affect transport to the interface [37,54–57]. Hence, similar to the discussions in Refs. [2–7,11,14], we interpret the above observations in terms of the nonlinear dynamics of coupled transport and surface kinetics. Since we found no impurity effects on the fluctuations, and an interfacial chemical reaction that is nonlinear in concentration is hard to envision, we conclude that the most likely model for our system is similar to that proposed that by Allegré, Provost, and Jaupart [4] (see Sec. I). In our case, the required delay in the interfacial kinetics response to perturbations in surface supersaturation σ_s can have various causes. In growth by 2D nucleation, due to the stochastic nature of this process, a local increase in σ_s does *not* result in an instantaneous appearance of a nucleus. On the other hand, dislocation-generated steps are often pinned at the outcrop points of other dislocations; see, e.g., Ref. [58]. Strong support of this interpretation comes from our parallel modeling efforts, in which we describe the stochastic generation of a large sequence of steps at the edge of the crystal and their subsequent motion across the interface according to the microscopic supersaturation resulting from diffusive solute transport. This model, evaluated with transport and kinetics parameters characteristic of lysozyme crystallization, quantitatively reproduces the amplitude and Δt's of the observed fluctuations [59].

Even without the benefit of the above detailed model, however, the relation between step bunch formation and sol-

ute supply toward the interface can be rationalized by a simple scaling argument. If bunching and transport are related, Δt should correspond to the time required to restore the interfacial supersaturation after the pasage of a macrostep. If transport close to the interface is dominated by diffusion, this time τ_D is of the order of

$$\tau_D = \delta^2/D, \tag{9}$$

where δ is the characteristic diffusion distance. This δ depends on the strength of the convective flow about the crystal. For this order of magnitude estimate, we take $\delta = 300$ μm [42]. Thus, we obtain from Eq. (9) $\tau_D \cong 1200$ s, which is in good agreement with the observed Δt. Note that this crude model also accounts for the observed decrease in Δt with increasing R. The steeper interfacial concentration gradient asociated with higher R's enhances convection and, thus, reduces δ.

On a microscopic level, we can compare our observations with the predictions of the step train stability analysis by Chernov and Nishinaga [27]. With $\Omega = 3\times10^{-20}$ cm^3 and $\alpha \cong 1$ erg/cm^2 [60,61], according to Eq. (2), the capillary length $\Gamma \approx 10^{-6}$ cm. Furthermore, with $R \cong 20$ Å/s [40], the face kinetic coefficient, defined as

$$\beta_f = R/(\Omega C s_b), \tag{10}$$

where $C = 2.1\times10^{18}$ cm^{-3} is the molecular concentration of the solution, becomes, with $s_b = 5$, $\beta_f \cong 10^{-6}$ cm/s. Approximating β_0 in Eq. (1) by this β_f, we obtain $\lambda_c \cong 30$ μm. Since perturbations can only affect crystals larger than their wavelength, equidistant step trains on crystals larger than 30 μm are unstable and step bunches should form. Since the interferometric measurements in our setup require crystals $\geqslant 100$ μm, we could not directly detect this limit. However, the average step bunching wavelength λ_0 should be of the order of $\lambda_{\max}$ of Eq. (3). In evaluating $\lambda_0 = \overline{\nu}\Delta t$ from Figs. 2–5, we see that this is the case.

As observed in Fig. 4, at higher supersaturations the fluctuation amplitude of R increases more than those of p and ν. This can also be understood in terms of transport considerations. Expanding $\nu(t)$ in Eq. (8), the growth rate R at any point on the interface can be written as

$$R(t) = p(t)b[p(t)]\sigma_s(t), \tag{11}$$

where $b(p)$ is a kinetic coefficient for incorporation of growth units into steps, and σ_s is the supersaturation at the interface. [For clarity, it should be noted that b is related to β_f of Eqs. (1)–(4) through $\beta_f = bp/\Omega C$.] In our system, $b(p)$ decreases with increasing p due to the overlap of the steps' (surface) diffusion fields; see Sec. III A. At low average growth rates, there is sufficient time after the passage of a step bunch for the local σ_s to recover. Hence the local σ_s is only insignificantly affected by variations in step density. As a consequence, the opposite deviations in p and $b(p)$ largely compensate, yielding a nearly steady R. At higher average R, however, the local σ_s is strongly modulated by the passing step bunches. This results in ν fluctuations that are out of phase with those in p, leading to pronounced nonsteady R.

More formally, the relation between the changes in the surface supersaturation and normal growth rate can be understood if one considers the time derivative of Eq. (11):

$$\frac{\partial R}{\partial t} = \left[\left(\frac{1}{p} + \frac{1}{b}\frac{\partial b}{\partial p} \right) \frac{\partial p}{\partial t} + \frac{1}{\sigma_s}\frac{\partial \sigma_s}{\partial t} \right] R, \tag{12}$$

or

$$\frac{1}{R}\frac{\partial R}{t} = \left(1 + \frac{p}{b}\frac{\partial b}{\partial p} \right) \frac{1}{p}\frac{\partial p}{\partial t} + \frac{1}{\sigma_s}\frac{\partial \sigma_s}{\partial t}. \tag{13}$$

Since

$$b(p) = b_0(1+kp)^{-1}, \tag{14}$$

where k is a (surface diffusion) step-field overlap parameter [50], and for our system

$$kp \gg 1 \tag{15}$$

[50,51] it follows that

$$\frac{p}{b}\frac{\partial b}{p} \approx -1. \tag{16}$$

Equation (16) reflects the observed compensation of the opposing p and ν fluctuations due to the strong interstep interaction expressed by Eq. (15). Thus the first term on the right hand side of Eq. (13) is vanishingly small, and

$$\frac{\partial R}{\partial t} \approx \frac{R}{\sigma_s}\frac{\partial \sigma_s}{\partial t}. \tag{17}$$

As a consequence, in the absence of σ_s modulations, R should be steady, even though p and ν fluctuate.

Furthermore, we can show that even under conditions that do not induce R fluctuations, step bunches that lead to variations in p may still form. From Eq. (13), with $\partial R/\partial t = 0$,

$$\frac{1}{p}\frac{\partial p}{\partial t} \approx \left(1 + \frac{p}{b}\frac{\partial b}{\partial p} \right)^{-1} \frac{1}{\sigma_s}\frac{\partial \sigma_s}{\partial t}. \tag{18}$$

In contrast to Eq. (17), the action of $(\partial\sigma_s/\partial t)$ upon $(\partial p/\partial t)$ is amplified by the large value of $[1+(p/b)(\partial b/\partial p)]^{-1}$ [see Eq. (16)]. Thus even small perturbations in σ_s, that do not result in significant R fluctuations, may lead to significant variations in local slope–step density. In addition, Eq. (18) helps to understand the significance of step field overlap for the macrostep formation, and ultimately, for the kinetics fluctuations. If the condition of Eq. (15) is not satisfied, $0 \geqslant (p/b)(\partial b/\partial p) \gg -1$, and small σ_s perturbations may only lead to insignificant p variations. This is similar to the interstep interaction effects on microscopic morphology formation on a much larger length scale. In the latter case, supersaturation nonuniformities of $\leqslant 10\%$ between facet center and edge induce up to fivefold increases in average slope [50,51].

C. Modification of step bunching by solutal convection

The increases in fluctuation amplitude with supersaturation and crystal size could indicate a dependence on super-

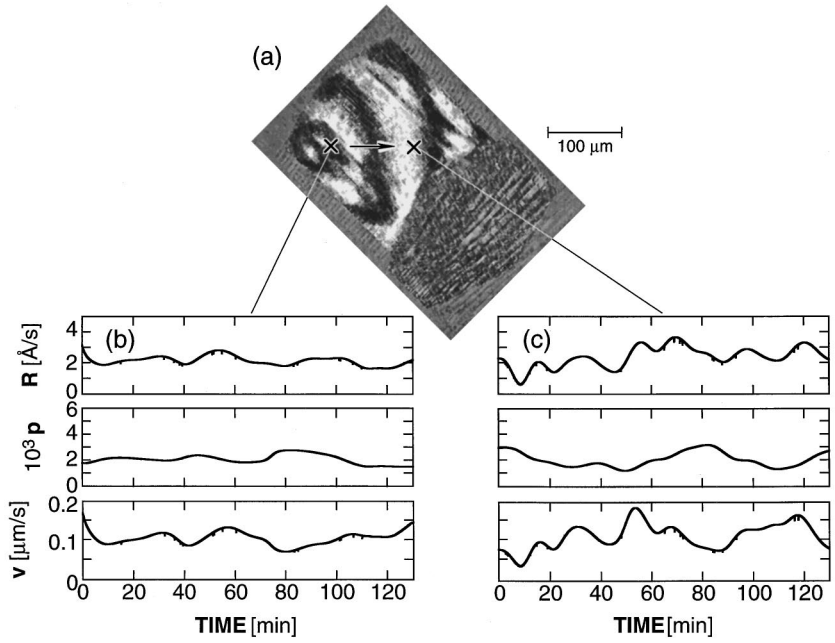

FIG. 6. Increase of fluctuation amplitude and step bunch height with distance from dislocation step source; $\sigma=1.64$. The arrow indicates the direction of step motion.

saturation nonuniformity which increases with both σ and a [54-56]. These observations could also indicate a role of buoyancy-driven convection, which, as mentioned above, also increases in strength with the larger density gradients resulting at higher σ (i.e., R) and larger a [37,57]. To distinguish between these possibilities, we investigated the dependence of the fluctuation amplitude on the direction of step motion with respect to the anticipated convective flow direction across the interface. In our experimental arrangement, the crystal rests on the bottom of the crystallization cell with the observed facet in horizontal orientation [13]. The growth-induced reduction in solute concentration at the interface results in a convection plume above the facet's center region [42,43,45]. Thus solution flows parallel to the interface from opposite edges toward the center, and then rises upward. As a consequence, steps originating in the center and edge regions move, respectively, against or in the direction of the flow.

Figures 6 and 7 show that the amplitude of the fluctuations, especially of p and ν, is substantially higher at the facet center, independent of the location of the dislocation step source. In similar observations on other crystals we found that this also holds for layer generation by 2D nucleation. Note, however, that as step bunches move from the edge to the center of the facet, the amplitude increases (Fig. 6). On the other hand, step motion toward the edge is associated with an amplitude decrease (Fig. 7). This differs from impurity-induced step bunching, where the height of the forming macrosteps is always expected to increase with distance from the step source; see, e.g., Refs. [62,63]. Note also that the observations in Fig. 7 support the conclusion made by evaluating Eq. (7), Sec. I, that the fluctuations do not represent solution-flow-induced step train instabilities. We see that fluctuations are present even with antiparallel step and solution flow directions, while solution flow causes mac-

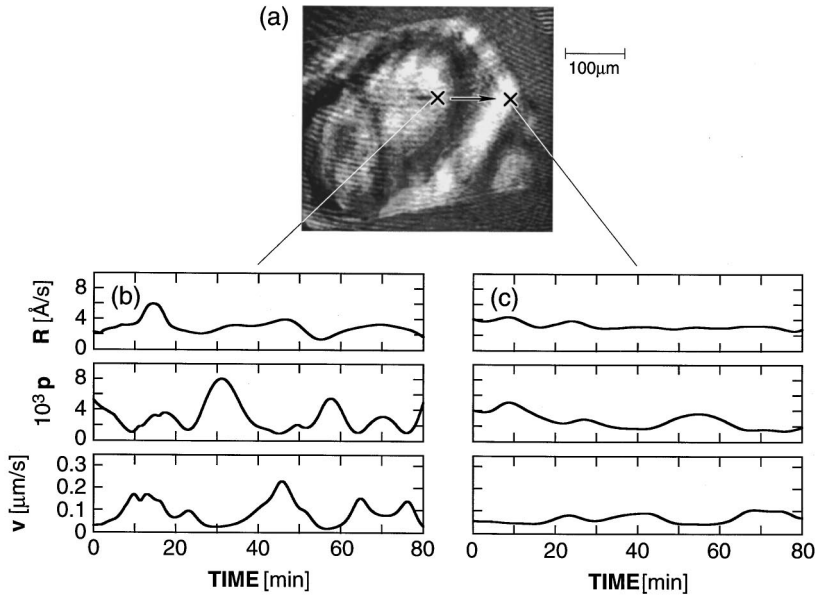

FIG. 7. Decrease of fluctuation amplitude and step bunch height with distance from dislocation step source; $\sigma=1.13$. The arrow indicates the direction of step motion.

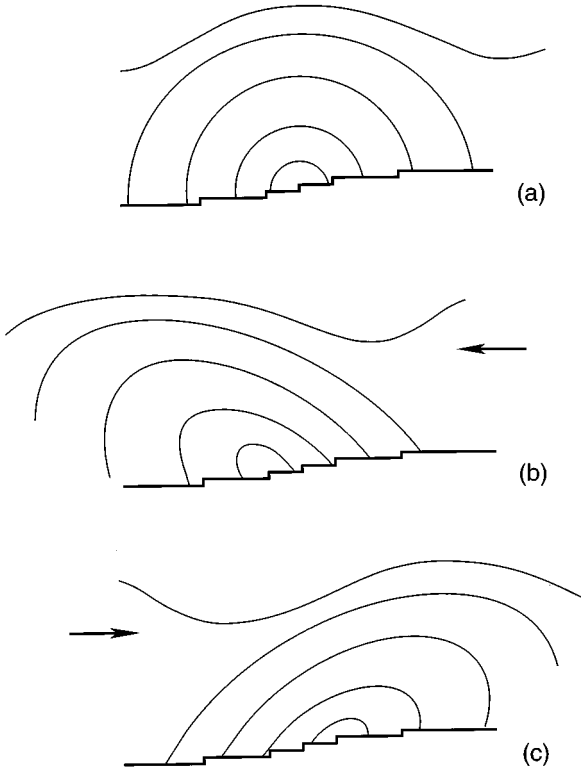

FIG. 8. Schematic illustration of solution flow effects on solute distribution (thin isoconcentration lines) over a step bunch (heavy profile): (a) no solution flow; (b) solution flow in the direction of step motion; (c) flow against step motion. Note the concentration gradient changes on the up- and down- flow sides of the bunch, and displacements of the concentration minimum.

rosteps only in the case of coinciding directions.

As was shown above [32–36], the dependence of the fluctuation amplitude on the direction of step motion can be understood in terms of convective transport effects. Evaluating Eqs. (5) and (6) in Sec. I, we predicted that buoyancy-driven convective flows should affect the development of step bunches in our system. Qualitatively, when the directions of the step train and flow motion coincide, the leading part of a step bunch is exposed to lower interfacial supersaturations and concentration gradients than the trailing one, as schematically illustrated in Fig. 8(b). Hence fewer steps leave the step bunch from the front than join it at the rear. This interaction between flow and kinetics further increases the number of elementary steps in a bunch resulting in a higher macrostep. However, during step propagation opposing the flow [Fig. 8(c)], σ_s and $|\mathbf{grad}C|$ are higher at the leading steps than at the trailing ones. Consequently, more steps leave the bunch than join it. This reduces the macrostep height *en route* across the interface.

If the above considerations apply to our system, step bunches moving from an edge of a facet through the center to the opposite edge and, thus, ''through'' the convection plume from parallel to antiparallel flow conditions, should first exhibit an increase and then a decrease in fluctuation amplitude. Figure 9 shows that this is the case.

For completeness, it must be mentioned that growth rate fluctuations could also be due to convective instabilities. Such instabilities associated with a convection plume have been observed in the solution growth of inorganic crystals; see, e.g., Ref. [64]. Likewise, as suggested by other solution growth experiments, it is possible that low growth rates [45], or, in particular, certain combinations of solutal and thermal density gradients [65], are associated with unsteady convective transport. Thus, nonsteady convection flows could possibly exist in the solution during our experiments. Yet the above directionality of the changes in fluctuation amplitude, as well as the observed amplitude dependence on the type of growth step source and crystal size, are difficult to interpret in terms of a unsteady bulk convection model.

IV. EFFECTS ON CRYSTAL PERFECTION

A. Fluctuation-induced striations

Figure 10 shows heavy veils in the (110) sectors of a lysozyme crystal grown from a Sigma solution. The forma-

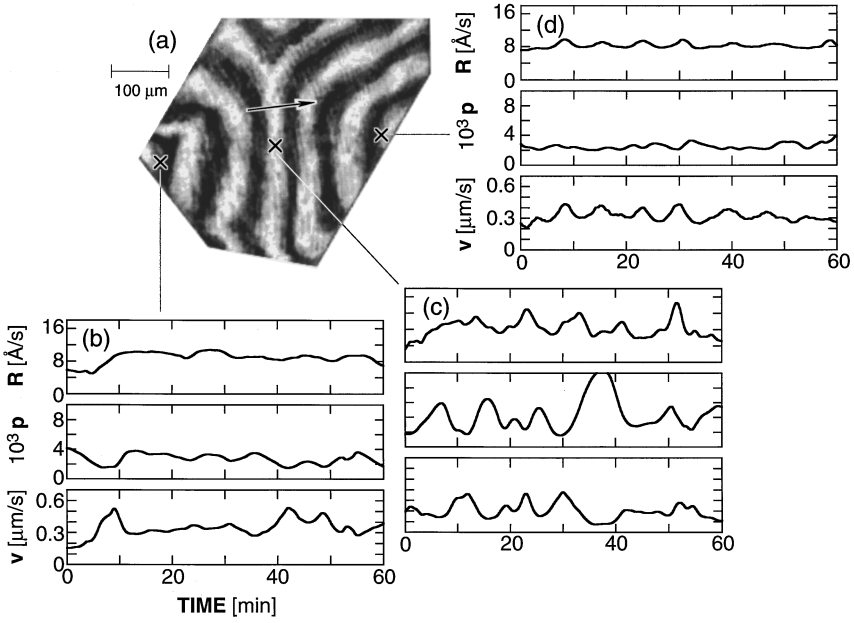

FIG. 9. Initial increase and subsequent decrease of fluctuation amplitude and step bunch height with distance from 2D nucleation step source; σ=2.84. The arrow indicates the direction of step motion.

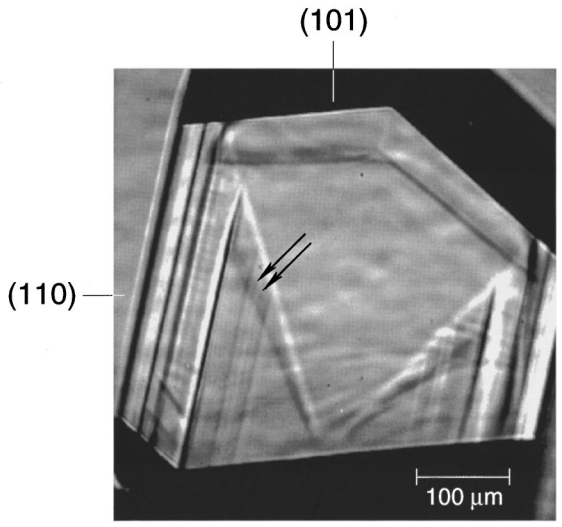

FIG. 10. Differential interference contrast micrograph of a crystal grown from Sigma solution at $2.2<\sigma<2.84$. Three heavy striations in the (110) sectors are caused by imposed $\Delta T=1$ °C [48]. Faint striations in between (T stable within 0.01 °C) are likely caused by intrinsic growth rate fluctuations.

tion of these veils was intentionally induced through temperature changes, as described in detail in Ref. [48]. Between these pronounced features, one notices faint striations. The spacing of these fine striations is of the order of micrometers. This coincides with the fluctuation length scale, i.e., the product of Δt and average R during growth under similar conditions; see Fig. 5. Although we have not demonstrated causality at this point, it appears that, similar to some vapor growth [8] and geochemical [2-4] systems, in lysozyme the growth kinetics fluctuations result in crystal striations and, thus, decrease the structural quality of the crystals. Moreover, from our observations one can expect some connection between the position of the steps sources on a facet, the orientation of that facet in the gravity field and the resulting structural quality in the corresponding growth sector.

B. Modification of nonlinear response through changes in transport conditions

About 20% of the proteins and viruses that were crystallized under reduced gravity yielded higher x-ray-diffraction resolution than their controls grown on Earth [66]. The remainder either showed no improvement, or diffracted to lower resolution either due to smaller sizes or, as documented for a few cases, lower crystal perfection [67]. Based on our findings, we can speculate on how changes in the transport conditions may affect the quality of the protein crystals or other systems with mixed transport-kinetics control. If, for instance, for the growth of a certain (protein) material on Earth, bulk transport and interfacial kinetics have comparable weights in overall rate control, its ''operating point'' lies near the maximum in Fig. 1. Then fluctuation amplitudes in response to perturbations may be significant. In this case, a shift of the working point to the right due to slower transport under low gravity conditions can dampen the fluctuations. This can result in higher crystal perfection. On the other hand, crystallization systems with slower surface kinetics and faster transport would operate in the left part of the diagram. Then, upon suppression of transport in space, fluctuation amplitudes may increase, and the crystal quality decrease.

The relative importance of transport and interface processes can be characterized by the kinetic Peclet number, Eq. (4) [68,69]. Values of $\mathrm{Pe}_k<0.1$ indicate dominant interfacial kinetics control, Pe_k's≥ 1 imply transport control. We evaluated Pe_k for four proteins that have been crystallized both on Earth and under reduced gravity, and for which the kinetic coefficients [40,41,70,71], as well as the diffusivities are known [44,72,73]. Of these, space-grown lysozyme and thaumatin crystals often diffract only to the resolution achievable on Earth (see, e.g., Refs. [74,75]). On the other hand, space-grown canavalin and satellite tobacco mosaic virus (STMV) crystals yielded higher diffraction resolution [76,77]. The Pe_k's of these systems are listed in Table I. The value for lysozyme and thaumatin reflect kinetics-dominated growth. For lysozyme, this is expected from earlier studies [41,42,48,78,79]. Hence, from the point of view of nonlinear response, an increase of transport's contribution to growth rate control under reduced gravity should not result in increased structural perfection. Observed exceptions [80] may have been the result of reduced impurity incorporation and/or the lack of sedimentation in space, see below. The Pe_k's for canavalin and the STMV indicate that these systems operate on Earth more in the mixed control regime than lysozyme. Hence we postulate that the higher perfection of space-grown crysytals of these materials is due to a reduction in nonlinear response, i.e., a shift of the working point toward transport control resulting from the diffusive transport at low gravity. Similarly, one may attempt to improve the perfection of (protein) crystals that, on Earth, grow in the mixed control regime, by moving their working point toward kinetics control by appropriate imposed solution flow. We are currently investigating this possibility.

Of course, besides the possible damping of growth rate fluctuations, there are other benefits for crystal perfection in space experiments. In the absence of buoyancy-driven convection, the interfacial concentration of slowly diffusing, growth-impeding impurities, can be substantially lower [46,77]. Furthermore, in space the sedimentation of foreign particles or microcrystals on a growing facet is reduced [76,77]. Note, however, that the mechanism put forth above provides a system-dependent rationale for advantages as well as disadvantages of reduced-gravity growth conditions for (protein) crystal perfection.

The nonlinear response of layer growth dynamics observed above may also underlie earlier observations in the growth of crystals on Earth. It has been widely recognized that the growth of homogeneous inorganic crystals, such as ammonium dihydrogen phosphate (ADP) requires intensive stirring of the nutrient solution. This can be interpreted in terms of the instability of equidistant step trains under diffusive transport conditions. As evaluated in Table I for typical growth conditions, the critical wavelength [see Eq. (1)] for ADP is of the order of 20 μm. Thus step bunching is unavoidable, and facets rapidly become covered by macrosteps, overhangs, and inclusions [30,81], unless, as discussed in Sec. I, one takes advantage of the stabilizing effect of forced convection on step trains that move opposite to the forced

TABLE I. Estimated critical wavelengths λ_c and kinetic Peclet numbers $Pe_k=\beta_f\delta/D$ of lysozyme, canavalin, the satellite tobacco mosaic virus (STMV), and ammonium dihydrogen phosphate (ADP) without and with forced solution flow. *Estimated value. †Evaluated from data in Refs. [40, 41]. ‡Evaluated from β_{step} using $\beta_{face}=|p|\beta_{step}{}^{h}$ with $p=10^{-2}$ [70]. §Evaluated from β_{step} using $\beta_{face}=|p|\beta_{step}{}^{h}$ with $p=3\times10^{-3}$ [38,39]. ‖ Evaluated using a characteristic diffusion length $\delta=300$ μm [37,42]. ¶Evaluated using a characteristic diffusion length $\delta=1$ μm (L. N. Rashkovich and B. Yu. Shekunov, Kristallografiya **35**, 160 (1990) [Sov. Phys. Crysytallogr. **35**, 96 (1990)]).

	Lysozyme	Thaumatin	Canavalin	STMV	ADP $u_\infty=0$	ADP $u_\infty=40$ cm/s
Molecular size (Å)	30[a]	35[b]	52[c]	160[d]	5	5
Mol. volume Ω (10^{-20} cm^3)	3[a]	6.5 [71]	41[e]	420[f]	0.01 [38,39]	0.01 [38,39]
D (10^{-6} cm^2/s)	0.73 [44]	0.6*	0.4 [72]	0.2 [73]	5.5[g]	5.5[g]
α (erg/cm^2)	1 [60,61]	?	?	1.5×10^{-2} [73,c]	29 [39]	29 [39]
β_{step} (cm/s)		2×10^{-4} [71]	5×10^{-4} [70]	8×10^{-4} [70]	0.4 [38,39]	0.4 [38,39]
β_f (cm/s)	1×10^{-6} †	2×10^{-6} ‡	5×10^{-6} ‡	8×10^{-6} ‡	1.2×10^{-3} §	1.2×10^{-3} §
λ_c (μm)	30‖			10‖	18‖	n.a.
$Pe_k=\beta_f\delta/D$	0.05‖	0.1‖	0.38‖	1.2‖	6.5‖	0.02¶

[a]C. C. F. Blake, D. F. Koenig, G. A. Mair, A. C. T. North, D. C. Phillips, and V. R. Sarma, Nature **206**, 757 (1965).
[b]T.-P. Ko, J. Day, A. Greenwood and A. McPherson, Acta Crystallogr. D **50**, 813 (1994).
[c]T.-P. Ko, J. D. Ng, and A. McPherson, Plant Physiol. **101**, 729 (1993).
[d]A. J. Malkin, J. Cheung, and A. McPherson, J. Cryst. Growth **126**, 544 (1993).
[e]T. A. Land, A. J. Malkin, Yu. G. Kuznetsov, A. McPherson, and J. J. De Yoreo, Phys. Rev. Lett **75**, 2774 (1995).
[f]A. J. Malkin, T. A. Land, Yu. G. Kuznetsov, A. McPherson, and J. J. De Yoreo, Phys. Rev. Lett. **75**, 2778 (1995).
[g]J. W. Mullin and A. Amatavivadhana, J. Appl. Chem. **20**, 153 (1970).
[h]A. A. Chernov, J. Cryst. Growth **24/25**, 11 (1974).

flow. Note that, since step trains move in various directions, optimum stabilization requires frequent reversal of the solution stirring direction. Although these considerations provide a consistent frame of interpretation, our results suggest that under mixed control conditions step bunching in solution growth may be more complex. In Table I, we evaluated Pe_k for the growth of ADP in unstirred and stirred solutions. One sees that without forced solution flow, rate control is mixed. This will likely lead to step bunching as a result of the nonlinear response of the system. On appropriate stirring, however, the system's operating point moves towards kinetics control, where the amplitude of potential fluctuations is reduced. This scenario provides a supplementary alternative to the earlier interpretations.

V. SUMMARY AND CONCLUSIONS

We have shown that, under all growth conditions studied, lysozyme growth kinetics fluctuate by as much as 80% of their average value, independent of solution purity. The associated variations in local slope (step density) indicate that the fluctuations occur through the dynamics of step bunching. The local slope and step velocity fluctuate approximately in counterphase, indicating strong step field overlap. Major excursions in the fluctuation amplitude are associated with the formation of compositional-structural striations.

The observed dependence of the fluctuation amplitude on supersaturation and crystal size, as well as the increased averaged frequencies at higher supersaturations, indicate that the unsteady growth is due to a higly nonlinear response of the system, that results in the mixed control regime from the coupling of solute bulk transport with nonlinear interface kinetics. The nonlinearity in kinetics may arise from the strong overlap of the step's supply fields, as well as from the delays in the response to interfacial supersaturation changes associated either with the random character of 2D nucleation or with the interaction between steps and dislocation outcrops.

Buoyancy-driven convection is not necessary for the generation of the fluctuations. However, convection significantly affects the effective macrostep height and fluctuation amplitude along the step pathway by altering the interfacial supersaturation distribution. If the direction of step motion is the same as that of convective flow, the fluctuation amplitude increases, while counterflow dampens the fluctuations.

Thus crystal quality may be improved by changing the ratio of transport to surface kinetics control by either enhancing or reducing transport in the solution. We speculate that this is one of the intrinsic reasons for the better quality of *some* of the protein crysytals grown under reduced gravity conditions. At the same time, this model provides a system-dependent rationale for advantages as well as disadvantages of reduced gravity for (protein) crystallization. Furthermore, these observations suggest that some of the step bunching observed in inorganic systems may also be due to nonlinear response of step dynamics in the mixed control regime.

ACKNOWLEDGMENTS

It is a pleasure to acknowledge numerous helpful suggestions and critical comments on the draft of the manuscript by A. A. Chernov. P. J. Ortoleva and A. J. Malkin kindly pro-

vided references. We have also benefitted from discussions with A. I. Fedoseyev, H. Lin, and V. Tonchev, and thank M. Alpaugh and B. R. Thomas for protein analyses and purification. L. A. Monaco participated in exploratory experiments. D. Bond helped with temperature stability measurements. L. Carver expertly prepared the figures. Support of this work was provided by NASA (Grant Nos. NAG8-950 and NAG8-1168) and the State of Alabama through the Center for Microgravity and Materials Research at the University of Alabama in Huntsville.

[1] F. Rosenberger, *Fundamentals of Crystal Growth, Vol. I: Macroscopic Equilibrium and Transport Concepts* (Springer, Berlin, 1979) p. 450.
[2] C. S. Haase, J. Chadam, D. Feinn, and P. Ortoleva, Science **209**, 272 (1980).
[3] P. J. Ortoleva, *Geochemical Self-Organization* (Oxford University Press, Oxford, 1994).
[4] C. J. Allègre, A. Provost, and C. Jaupart, Nature **294**, 223 (1981).
[5] H. U. Walter, J. Electrochem. Soc. **123**, 1098 (1976).
[6] J. J. Favier, J. Electrochem. Soc. **129**, 2355 (1982).
[7] M. Koper, *Far-From-Equilibrium Phenomena in Electrochemical Systems, Instabilities, Oscillations and Chaos* (University of Utrecht Press, Utrecht, The Netherlands, 1994).
[8] M. Piechotka, J. Cryst. Growth **146**, 1 (1995).
[9] B. Yu. Shekunov, L. N. Rashkovich, and I. L. Smol'skii, J. Cryst. Growth **116**, 340 (1992).
[10] K. Onuma, T. Kameyama, and K. Tsukamoto, J. Cryst. Growth **137**, 610 (1994).
[11] J. M. Garcia-Ruiz, A. Santos, and E. J. Alfaro, J. Cryst. Growth **84**, 555 (1996).
[12] R. I. Ristic, B. Shekunov, and J. N. Sherwood, J. Cryst. Growth **160**, 330 (1996).
[13] P. G. Vekilov, L. A. Monaco, and F. Rosenberger, J. Cryst. Growth **148**, 289 (1995).
[14] B. Caroli, C. Caroli, and B. Roulet, J. Phys. (Paris) **44**, 945 (1983).
[15] S. R. Corriel and R. F. Sekerka, J. Cryst. Growth **61**, 499 (1983).
[16] S. Harris, J. Cryst. Growth **135**, 354 (1994).
[17] R. M. Noyes and R. J. Fields, Ann. Rev. Phys. Chem. **25**, 95 (1974).
[18] F. Argoul, A. Arneodo, P. Richeti, and J. C. Roux, J. Chem. Phys. **86**, 3325 (1987); **86**, 3339 (1987).
[19] P. Gray and S. K. Scott, *Chemical Oscillation and Instabilities. Non-linear Chemical Kinetics* (Clarendon, Oxford, 1990).
[20] I. Sunagawa and P. Bennema, in *Preparation and Analysis of Solid State Materials*, edited by W. R. Wilcox (Marcel Decker, New York, 1982), Vol. 7, p. 1.
[21] I. Sunagawa, in *Materials Science of the Earth's Interior*, edited by I. Sunagawa (Terra, Tokyo, 1984), pp. 303 and 323.
[22] I. Sunagawa and P. Bennema, J. Cryst. Growth **46**, 451 (1979).
[23] C. van Leeuven, R. van Rosmalen, and P. Bennema, Surf. Sci. **44**, 213 (1974).
[24] M. Uwaha, Y. Saito, and M. Sato, J. Cryst. Growth **146**, 164 (1995).
[25] Y. Saito and M. Uwaha, Phys. Rev. B **51**, 11 172 (1995).
[26] R. L. Schwoebel and E. J. Shipsey, J. Appl. Phys. **37**, 3682 (1966).
[27] A. A. Chernov and T. Nishinaga, in *Morphology of Crystals*, edited by I. Sunagawa (Terra, Tokyo, 1987), p. 207.
[28] V. G. Levich, *Physicochemical Hydrodynamics* (Prentice Hall, Englewood Cliffs, NJ, 1962).
[29] A. A. Chernov, Usp. Fiz. Nauk. **73**, 277(1961) [Sov. Phys. Usp. **4**, 116 (1961)].
[30] A. A. Chernov, *Modern Crystallography, Vol. III: Growth of Crystals* (Springer, Berlin, 1984), p. 246.
[31] L. N. Rashkovich and B. Yu. Shekunov, J. Cryst. Growth **100**, 133 (1990).
[32] A. A. Chernov, Yu. G. Kuznetsov, I. L. Smol'skii, and V. N. Rozhanskii, Kristallografiya **31**, 1193 (1986) [Sov. Phys. Crystallogr. **31**, 705 (1986)].
[33] A. A. Chernov, J. Cryst. Growth **118**, 333 (1992).
[34] A. A. Chernov, S. R. Corriel, and B. T. Murray, J. Cryst. Growth **132**, 405 (1993).
[35] S. Yu. Potapenko, J. Cryst. Growth **147**, 223 (1995).
[36] S. Yu. Potapenko, J. Cryst. Growth **158**, 346 (1995).
[37] H. D. Yoo, W. R. Wilcox, R. B. Lal, and J. D. Trolinger, J. Cryst. Growth **92**, 101 (1988).
[38] P. G. Vekilov, Yu. G. Kuznetsov, and A. A. Chernov, J. Cryst. Growth **121**, 643 (1992).
[39] P. G. Vekilov, Yu. G. Kuznetsov, and A. A. Chernov, J. Cryst. Growth **121**, 44 (1992).
[40] P. G. Vekilov and F. Rosenberger, J. Cryst. Growth **158**, 540 (1996).
[41] P. G. Vekilov, M. Ataka, and T. Katsura, Acta Crystallogr. D **51**, 207 (1995).
[42] H. Lin, F. Rosenberger, J. I. D. Alexander, and A. Nadarajah, J. Cryst. Growth **151**, 153 (1995).
[43] M. Pusey, W. Witherow, and R. Naumann, J. Cryst. Growth **90**, 105 (1988).
[44] M. Muschol and F. Rosenberger, J. Chem. Phys. **103**, 10 424 (1995).
[45] K. Onuma, K. Tsukamoto, and I. Sunagawa, J. Cryst. Growth **89**, 177 (1988).
[46] F. Rosenberger, P. G. Vekilov, M. Muschol, and B. R. Thomas, J. Cryst. Growth **168**, 1 (1996).
[47] F. Rosenberger, S. B. Howard, J. W. Sowers, and T. A. Nyce, J. Cryst. Growth **129**, 1 (1993).
[48] L. A. Monaco and F. Rosenberger, J. Cryst. Growth **129**, 465 (1993).
[49] B. R. Thomas, P. G. Vekilov, and F. Rosenberger, Acta Crystallogr. D **52**, 776 (1996).
[50] P. G. Vekilov, L. A. Monaco, and F. Rosenberger, J. Cryst. Growth **156**, 267 (1995).
[51] H. Lin, P. G. Vekilov, and F. Rosenberger, J. Cryst. Growth **158**, 552 (1996).
[52] W. K. Burton, N. Cabrera, and F. C. Frank, Philos. Trans. R. Soc. London Ser. A **243**, 299 (1951).
[53] P. G. Vekilov and Yu. G. Kuznetsov, J. Cryst. Growth **119**, 248 (1992).
[54] A. Seeger, Philos. Mag. **44**, 348 (1953).

[55] W. R. Wilcox, J. Cryst. Growth **37**, 229 (1977).
[56] W. R. Wilcox, J. Cryst. Growth **38**, 73 (1977).
[57] W. R. Wilcox, J. Cryst. Growth **65**, 133 (1983).
[58] J. J. De Yoreo, T. A. Land, and B. Dair, Phys. Rev. Lett. **73**, 838 (1994).
[59] P. G. Vekilov, H. Lin, and F. Rosenberger, Phys. Rev. E (to be published).
[60] P. G. Vekilov, L. A. Monaco, B. R. Thomas, V. Stojanoff, and F. Rosenberger, Acta Crystallogr. D **52**, 785 (1996).
[61] A. A. Chernov and H. Komatsu, in *Science and Technology of Crystal Growth*, edited by J. P. van der Eerden and O. S. L. Bruinsma (Kluwer, Amsterdam, 1995), p. 329.
[62] J. P. van der Eerden and H. Müller-Krumbhaar, Electrochim. Acta **31**, 1007 (1986).
[63] J. P. van der Eerden and H. Müller-Krumbhaar, Phys. Rev. Lett. **57**, 2431 (1986).
[64] K. Onuma, K. Tsukamoto, and I. Sunagawa, J. Cryst. Growth **98**, 384 (1989).
[65] F. Rosenberger, *Fundamentals of Crystal Growth, Vol. I: Macroscopic Equilibrium and Transport Concepts* [Ref. [1]], p. 380.
[66] L. J. DeLucas *et al.*, J. Cryst. Growth **135**, 183 (1994).
[67] R. Hilgenfeld, A. Liesum, R. Storm, and A. Plaas-Link, J. Cryst. Growth **122**, 330 (1992).
[68] A. A. Chernov, Kristallografiya **16**, 842 (1971) [Sov. Phys. Crystallogr. **16**, 734 (1972)].
[69] W. R. Wilcox, in *Preparation and Properties of Solid State Materials, Vol. I: Aspects of Crystal Growth*, edited by R. E. Lefever (Marcel Dekker, New York, 1971) p. 37.
[70] A. McPherson, A. J. Malkin, and Yu. G. Kuznetsov, Structure **3**, 759 (1995).
[71] A. J. Malkin, Yu. G. Kuznetsov, W. Glantz, and A. McPherson, J. Phys. Chem. **100**, 11 736 (1996).
[72] W. Kadima, A. McPherson, M. F. Dunn, and F. Jurnak, Biophys. J. **57**, 125 (1990).
[73] A. J. Malkin and A. McPherson, J. Cryst. Growth **126**, 555 (1993).
[74] M. C. Vaney, S. Maigan, M. Riès-Kautt, and A. Ducruix, Acta Crystallogr. Sect. D **52**, 505 (1996).
[75] A. J. Malkin and A. McPherson (private communication).
[76] Alexander McPherson, in *Proceedings of the VIIIth European Symposium on Materials and Fluid Science in Microgravity*, edited by J. C. Legros (University of Brussels, Brussels, 1992), Vol. 2, p. 619.
[77] A. McPherson, J. Phys. D **26**, 104 (1993).
[78] S. Miyashita, H. Komatsu, and Y. Suzuki, Jpn. J. Appl. Phys. **32**, 1855 (1993).
[79] S. Miyashita, H. Komatsu, Y. Suzuki, and T. Nakada, J. Cryst. Growth **141**, 419 (1994).
[80] E. H. Snell, S. Weisgerber, J. R. Helliwell, F. Weckert, K. Hölzer, and R. Schroer, Acta Crystallogr. D **51**, 1099 (1995).
[81] Yu. G. Kuznetsov and P. G. Vekilov (unpublished).